Analytical and Bioanalytical Chemistry (2023) 415:1287–1298
https://doi.org/10.1007/s00216-022-04248-4

PAPER IN FOREFRONT

Single-particle assessment of six different drug-loading strategies for incorporating doxorubicin into small extracellular vesicles

Chen Chen[1] · Yurou Li[1] · Qingqing Wang[1] · Niangui Cai[1] · Lina Wu[1] · Xiaomei Yan[1]

Received: 23 June 2022 / Revised: 15 July 2022 / Accepted: 21 July 2022 / Published online: 10 August 2022

Abstract

Extracellular vesicles (EVs) have emerged as an attractive drug delivery system owing to their natural roles in intercellular communication. On account of the large intrinsic heterogeneity of EVs, it is highly desirable to evaluate not only the encapsulation efficiency but also the alteration of biological functionality after the drug-loading process at the single-particle level. However, the nanoscale size of EVs poses a great challenge. Taking advantage of nano-flow cytometry (nFCM) in the multiparameter analysis of single EVs as small as 40 nm, six commonly used drug-loading strategies (coincubation, electroporation, extrusion, freeze-thawing, sonication, and surfactant treatment) were exploited by employing doxorubicin (Dox) as the model drug. Encapsulation ratio, EV concentration, drug content, and membrane proteins of Dox-loaded EVs were measured at the single-particle level. Our data indicated that coincubation and electroporation outperformed other methods with an encapsulation ratio of approximately 45% and a higher Dox content in single EVs. Interestingly, the labeling ratios of membrane proteins indicated that varying degrees of damage to the surface proteins of EVs occurred upon extrusion, freeze-thawing, sonication, and surfactant treatment. Confocal fluorescence microscopy and flow cytometry analysis revealed that Dox-loaded EVs prepared by electroporation induced the strongest apoptosis followed by coincubation. These results correlated well with their cellular uptake rate and fundamentally with the Dox encapsulation efficiency of single EVs. nFCM provides a rapid and sensitive platform for single-particle assessment of drug-loading strategies for incorporating drugs into EVs.

Keywords Extracellular vesicles · Single-particle analysis · Drug-loading strategy · Doxorubicin · Nano-flow cytometry

Introduction

Extracellular vesicles (EVs) are nanoscale lipid membranes (40–1000 nm in diameter, with majority of them smaller than 200 nm and termed as sEVs) secreted by cells to shuttle functional biological molecules such as proteins, nucleic acids, and lipids for intercellular communication [1–5]. Owing to the excellent biocompatibility, long circulation time, and inherent targeting ability, EVs have shown great potential in serving as a drug delivery system [6, 7]. Currently, most of the drugs are loaded into EVs via post-loading strategies [8–10], of which EVs are isolated first and then drugs are incorporated by simple coincubation, electroporation, extrusion, freeze-thawing, sonication, or transient membrane permeabilization [11–13]. Post-loading is direct and also suitable for loading EVs from various sources, including plant cells and milk [14, 15]. For the treatment of different diseases, a variety of drug molecules including antitumor drugs, enzymes, small interfering RNA (siRNA), and microRNA (miRNA) could be loaded into EVs. For example, Kamerkar et al. prepared siRNA-loaded EVs by electroporation for therapeutic targeting of oncogenic KRAS in pancreatic cancer, achieving obvious tumor suppression and higher survival in a mouse model [16].

Published in the topical collection *Advances in Extracellular Vesicle Analysis* with guest editors Lucile Alexandre, Jiashu Sun, Myriam Taverna, and Wenwan Zhong.

✉ Xiaomei Yan
xmyan@xmu.edu.cn

[1] Department of Chemical Biology, The MOE Key Laboratory of Spectrochemical Analysis & Instrumentation, The Key Laboratory for Chemical Biology of Fujian Province, Collaborative Innovation Center of Chemistry for Energy Materials, Department of Chemical Biology, College of Chemistry and Chemical Engineering, Xiamen University, Xiamen 361005, People's Republic of China

Haney et al. reported that macrophage-derived EVs can be loaded with catalase for Parkinson's disease [17]. In addition, small-molecule chemotherapeutics, including paclitaxel, doxorubicin (Dox), and methotrexate, have also been employed for EV-based therapy for anti-tumor treatment [18].

Although EV-based drug delivery systems have many unique advantages and broad application prospects, systematic study is lacking for efficient loading of small-molecule drugs into EVs. Due to the distinct physicochemical properties of different drugs, correspondingly optimized loading strategies need to be selected while taking these factors into consideration: drug-loading efficiency, vesicle integrity, and function maintenance of surface proteins. In view of the extremely tiny size of EVs and the low content of encapsulated drugs, most studies used ensemble-averaged methods to evaluate the effectiveness of drug loading into EVs [12, 19]. However, EVs are highly heterogeneous and existing approaches cannot differentiate whether drugs are specifically associated with EVs or reside instead in the solution phase despite the post-separation efforts to remove excess drugs (e.g., ultracentrifugation or size-exclusion chromatography) [20, 21]. Therefore, assessing drug-loaded EVs at the single-particle level is highly demanded to address these challenges for optimal performance and good quality control [19, 22, 23].

By integrating strategies for single-molecule fluorescence detection in a sheathed flow with light scattering detection, our laboratory has developed nano-flow cytometry (nFCM). The particle size, drug quantity and loading efficiency, and ligand density of lipid-based nanomedicines have been characterized at the single-particle level [9, 24, 25]. In particular, the particle size, purity, protein profile, drug content, and EV-DNA have been analyzed for single EVs as small as 40 nm [26–31]. In this work, we report the application of nFCM for the single-particle assessment of six different drug-loading strategies for EVs by using Dox as the model drug. This is not only because Dox is a widely used anti-cancer drug but also because it is fluorescent, so that the drug fluorescence signal can be used as the direct reporter for drug quantity loaded into single EVs. Encapsulation ratio (defined as the percentage of drug-loaded EVs to all the EVs), EV concentration, Dox content, and membrane protein level were measured for Dox-loaded EVs at the single-particle level. The impact of different storage conditions on preserving the encapsulation efficiency of Dox-loaded EVs was also investigated. Moreover, the drug encapsulation efficiency (taking both the encapsulation ratio and drug content in single EVs into account) correlated well with the cell apoptosis rates, confirming the effectiveness of using nFCM for drug-loading characterization of EVs.

Materials and methods

Cell culture

The human colorectal cancer cell line (HCT-15) and the human embryonic kidney cell line (HEK293T) were purchased from American Type Culture Collection (ATCC). HEK293T cells were cultured in DMEM medium (Gibco), and HCT-15 cells were cultured in RPMI 1640 medium (Gibco). All media were supplemented with 10% FBS and penicillin–streptomycin (Invitrogen). The FBS (ExCell Bio, FSP500) used above was depleted of EVs by ultracentrifugation at 100,000 × g for 18 h at 4 °C (Beckman Coulter X-90 centrifuge, SW41 Ti rotor).

Isolation and purity assessment of EVs

Cells were grown in EV-depleted medium until they reached a confluence of approximately 90% (after approximately 24 h). EV isolation by differential ultracentrifugation was performed as described in our previous work [26, 30]. Briefly, the conditioned cell culture medium (CCCM) was collected and centrifuged at 800 × g for 5 min at 4 °C to pellet the cells. The supernatant was centrifuged at 2000 × g for 10 min at 4 °C to remove cellular debris. Freshly prepared CCCM of HEK293T cells (12.5 mL) were centrifuged at 100,000 × g for 2 h at 4 °C in a Beckman Coulter XE-90 K Ultracentrifuge using an SW41 Ti rotor. The pellet was washed with 12.5 mL of PBS and followed by a second ultracentrifugation at 100,000 × g for 2 h at 4 °C. Afterwards, the supernatant was discarded and the EVs were resuspended in 50 µL PBS. All PBS used in this paper have been filtered through a 220-nm filter. For the purity assessment experiment, to 45 µL of the EV preparation with a particle concentration of approximately 1.5×10^{10} particles/mL, 5 µL of 10% Triton X-100 (Sigma-Aldrich) was added. After 30 min incubation at room temperature, the treated sample was diluted tenfold prior to the nFCM analysis.

Dox-loading procedures

Dox loading in EVs was achieved by coincubation, electroporation, extrusion, freeze-thawing, sonication, Triton X-100 treatment, and Tween-20 treatment. For coincubation, 100 µL EVs of ~ 3×10^{10} particles/mL was added to 100-µL Dox solutions to

make the final Dox concentration of 5, 10, 25, 50, 100, 200, 250, or 300 μM. The mixture was incubated for 1 h at 37 °C. With regard to the other loading methods, 100 μL EVs of ~ 3×10^{10} particles/mL was mixed with 100 μL of 200-μM Dox solution for comparison. For electroporation, the mixture was pulsed at 400 V in a 4-mm cuvette by a Gene Pulser Electroporator (Bio-Rad), according to literature reports with minor modification [16]. For extrusion, the mixture was extruded through 200-nm polycarbonate (PC) membranes for 10 cycles at room temperature (RT). For freeze-thawing, the mixture was subjected to 3 freeze–thaw cycles between − 80 and 37 °C water bath. For sonication, the mixture was sonicated using a Zealway Ultrasonicator (Model S04H) under the following settings: 30% amplitude and 20 s on/off for 2 min at RT. For Triton X-100 treatment, the EVs and Dox mixture, containing 0.1% Triton X-100, was incubated at RT for 10 min. For Tween-20 treatment, the EVs and Dox mixture, containing 0.1% Tween-20, was incubated at RT for 10 min. After the loading procedure, EVs were washed twice with 1 mL PBS by ultracentrifugation at 100,000 × g for 17 min at 4 ℃ (Beckman Coulter MAX-XP centrifuge, TLA-120.2 rotor) [30]. The pellet was resuspended in 50 μL PBS for nFCM analysis. It was noted that centrifuging at 100,000 × g for 17 min with a Beckman Coulter Optima Max-XP ultracentrifuge equipped with a TLA 120.2 rotor offers the same fractionation effect as that of centrifuging at 100,000 × g for 120 min with a Beckman Coulter XE-90 K ultracentrifuge equipped with an SW41 Ti rotor (https://www.mybeckman.uk/centrifuges/rotors/calculator).

nFCM analysis

The laboratory-built nFCM reported before was used in the present study [26, 27, 30]. Briefly, two single-photon counting avalanche photodiodes (APDs) were used for the simultaneous detection of the side scatter light (SSC, a FF01 – 524/24 bandpass filter for a 532-nm laser) and fluorescence (FL, FF01 – 579/34 bandpass filter for orange fluorescence) of individual EVs, respectively. Unless stated otherwise, each distribution histogram or dot plot was derived from data collected 1 min. Ultrapure water supplied by an ultrapure water system (PURELAB Ultra FLC00006307, ELGA) served as the sheath fluid via gravity feed.

For nFCM analysis, the sample stream is completely illuminated within the central region of the focused laser beam, and the detection efficiency is approximately 100%, which leads to accurate particle concentration measurement via single-particle enumeration [32, 33]. The concentration of an EV sample (C_E) was determined by employing 100-nm orange FluoSpheres of known particle concentration to calibrate the sample flow rate. Several dilutions were made to the orange FluoSpheres solution, and a linear correlation between particle concentration and detected event rate was obtained with an R^2 of 0.999 (data not shown). For particle size measurement of EV preparations, a mixture of monodispersed silica nanoparticles (SiNPs) of five different diameters ranging from 47 to 123 nm (47, 59, 74, 95, and 123 nm) was analyzed using nFCM at the same instrument settings as those used for EV analysis. Considering the refractive index difference between the SiNPs (1.463) and EVs (1.400) at 532 nm excitation, the intensity ratio between light scattered by a SiNP to that of an EV of the same particle size was calculated based on the Mie theory for every size of the SiNP standard. These ratios were used as the correction factors to derive the calibration curve between the scattered light intensity and particle size of EVs from the data of SiNPs [26, 27].

Digestion of external EV-DNA and EV-DNA staining

For the digestion of external EV-DNA, approximately 1.5×10^{10} particles/mL of blank EV or Dox-loaded EV preparation was treated with 0.2-U/μL RNase-free DNase I (Takara, 2270A) for 30 min at 37 ℃. For EV-DNA staining, a 100-μL aliquot of the EV preparation with a particle concentration of ~ 1.5×10^{10} particles/mL was stained with 6 μM SYTO 82 (Thermo Fisher, S11363) for 20 min at 37 ℃. Tenfold dilution with 6 μM SYTO 82 was conducted prior to the nFCM analysis.

Immunofluorescent staining

Immunofluorescent staining for nFCM analysis was conducted following the procedures described in our previous work [30]. PE-conjugated mouse anti-human CD24 antibody (clone ML5), PE-conjugated mouse anti-human CD47 antibody (clone CC2C6), PE-conjugated mouse anti-human CD63 antibody (clone H5C6), and PE-conjugated mouse IgG1, κ (clone MOCP-21) were purchased from BD Biosciences. Into each 50-μL EV preparation with a particle concentration of ~ 1.5×10^{10} particles/mL, 20 μL of PE-conjugated antibody against CD24, CD47, or CD63 was added. The mixture was incubated at 37 ℃ for 30 min and then washed twice with 1 mL PBS by ultracentrifugation at 100,000 × g for 17 min at 4 ℃ (Beckman Coulter MAX-XP centrifuge, TLA-120.2 rotor). The pellet was resuspended in 50 μL PBS for nFCM analysis.

Drug-loading assessment by microplate reader

Dox-loaded EVs (50 μL, approximately of 1.5×10^{10} particles/mL) were lysed thoroughly using Triton X-100 essays and transferred into a 96-well plate. Then a SpectraMax iD5 microplate reader was used to measure the fluorescence emission of Dox at 580 nm ($E_{580\,nm}$). The particle concentration C_E was measured by nFCM as mentioned above. The Dox-loading quantity per single EV ($Mean_{Dox}$) was calculated by using the following formula:

$\text{Mean}_{\text{Dox}} = E_{580\,\text{nm}}/C_{\text{E}}$.

Cellular internalization and apoptosis analysis

For intracellular uptake studies, approximately 1×10^8 Dox-loaded EVs were incubated with 1×10^5 HCT-15 cells in a 12-well plate or 15-mm culture dish. For confocal microscopy measurements, after a 4-h incubation, the uninternalized EVs were removed. The cells were washed with PBS and fixed with 4% (v/v) paraformaldehyde (Sigma-Aldrich) for 15 min at RT. The cells were then washed with PBS, stained with Hoechst 33,342, and imaged on a Leica SP8 confocal microscope. For FCM analysis, the cells were washed by 800 g centrifugation after a 12-h incubation. The fluorescence intensity of the cells was measured immediately by a BD FACSAria III cytometer. For apoptosis analysis, an FITC Annexin V Apoptosis Detection Kit (BD Biosciences) was used for apoptosis measurements according to the manufacturer's specification.

Results

Experimental design and characterization of HEK293T EVs

We attempted to investigate six different drug-loading strategies for incorporating Dox into EVs by nFCM, including simple coincubation, electroporation, extrusion, freeze-thawing, sonication, and surfactant treatment. An anti-tumor drug Dox, which has been widely reported in researches of EV therapy, was selected as the model cargo for EV encapsulation in this study. As depicted in Fig. 1, both the SSC and the Dox fluorescence signals of individual Dox-loaded EVs were detected simultaneously with an analysis rate up to 10,000 particles per minute. The features of encapsulation ratio, particle concentration, drug content, and surface proteins were measured for each loading method.

As shown in Fig. 2a, EVs were isolated from HEK293T cells by differential centrifugation and ultracentrifugation. The isolated EVs were characterized extensively following the recommendations of the International Society for Extracellular Vesicles [34]. TEM images shown in Fig. 2b indicate that vesicles exhibited typical cup shapes. Western blotting analysis showed the presence of CD9 and syntenin along with the absence of calnexin proteins in the EV preparation (Fig. 2c). The SSC distribution histograms measured by nFCM for the EV preparation before and after Triton X-100 treatment are displayed in Fig. 2d. Figure 2e indicates that the events detected in 1 min reduced from 6098 to 1287 upon membrane lysis of EVs, and the purity of EVs was calculated to be ~ 80%. Figure 2f shows the SSC distribution histogram of a mixture of 47-, 59-, 74-, 95-, and 123-nm SiNPs. When the centroids of the SSC intensity obtained from the fitted Gaussian curves were corrected for each size population of the SiNPs based on the Mie theory, a calibration curve of the SSC intensity and the particle size of EVs can be obtained (Fig. 2g). Then the particle size of each individual EVs can be derived from its SSC intensity, and the particle size distribution histogram of HEK293T EVs is shown in Fig. 2h. The diameter of the isolated EVs was generally smaller than 220 nm, with the peak and median size identified to be 52 nm and 103 nm, respectively. All these results indicate a good recovery of EVs from cell culture supernatant.

Analysis of Dox-loading capacity by nFCM

After identifying the purity of isolated EVs, we then loaded Dox into EVs using different strategies. The Dox-loaded EVs were analyzed by nFCM through simultaneous SSC and FL detection of single particles as they passed sequentially through the focused laser beam of nFCM. Figure 3a shows the representative burst traces of SSC and FL signals of native EVs and Dox-loaded EVs by incubating EVs with 100 μM Dox for 1 h at 37 °C. Compared to native EVs of which only SSC signal was observed, concurrent FL signal

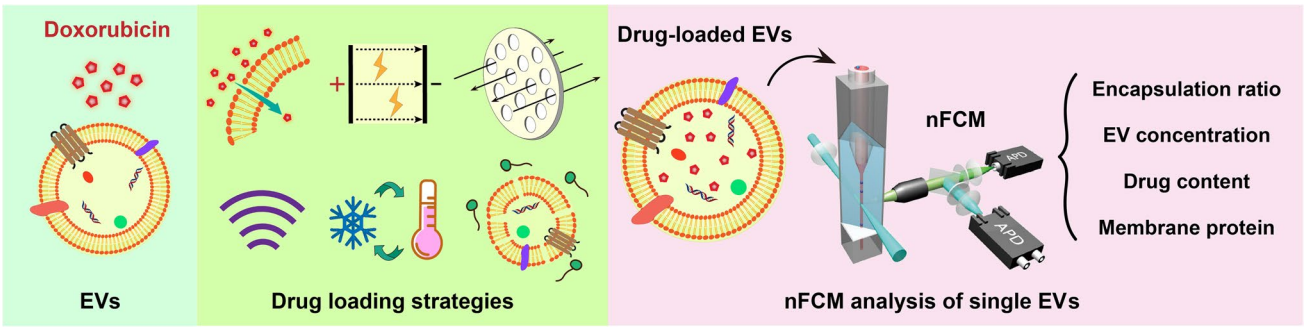

Fig. 1 Schematic diagram of applying single EV analysis by nFCM for the assessment of different doxorubicin loading strategies

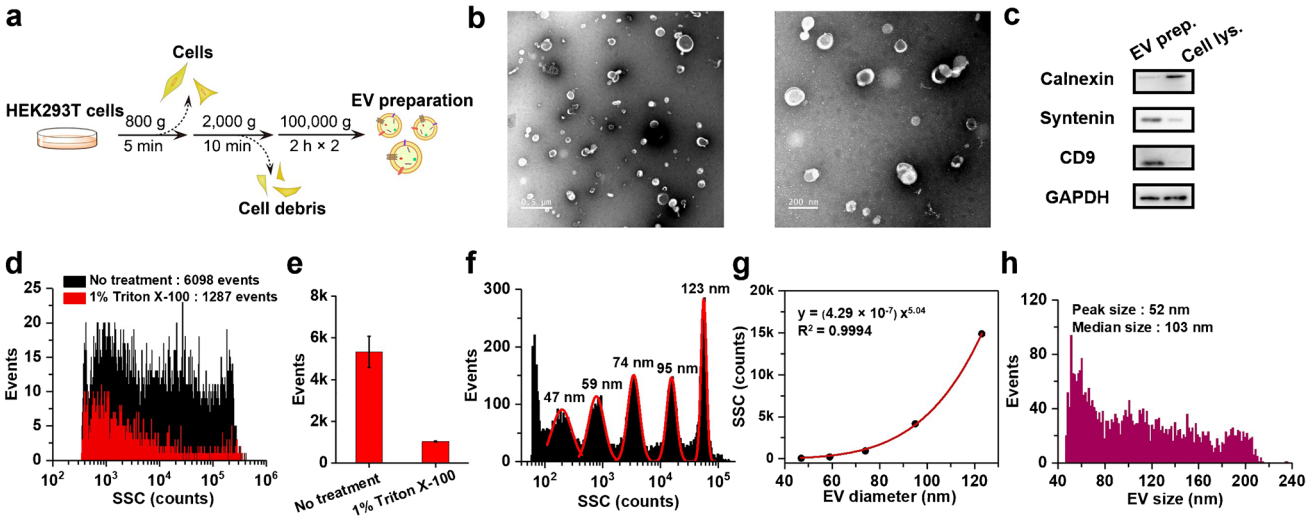

Fig. 2 Characterization of HEK293T EVs. **a** Isolation procedure of HEK293T EVs from cell culture supernatant. **b** Representative TEM micrographs of an EV isolate; the scale bars are 500 nm and 200 nm, respectively. **c** Immunoblots of a cell lysate and an EV preparation. **d** SSC distribution histograms for an EV preparation before (black line) and after (red line) Triton X-100 treatment. **e** The bar graph of event rate detected in 1 min for both samples, and the error bar represents the standard deviation (s.d.) of three replicate experiments. **f** SSC distribution histogram of a mixture of monodisperse SiNPs of five different diameters ranging between 47 and 123 nm, and fit to a sum of Gaussian peaks. **g** Plot of the Gaussian-fitted SSC intensity (after refractive index correction) as a function of EV particle size. **h** Histogram of particle size with a bin width of 1 nm for an EV sample isolated from cell culture supernatant of HEK293T cells by ultracentrifugation

was detected for most of the particles for the preparation of Dox-loaded EVs. The bivariate dot plot of Dox fluorescence versus SSC shows a 46.3% of encapsulation ratio, and EVs exhibiting Dox fluorescence were mainly large-size EVs with bright SSC signal (Fig. 3b). TEM image shows that the integral membrane structure was maintained upon Dox loading via coincubation (Fig. 3c). The statistically representative SSC and FL distribution histograms of EVs without or with Dox loading are shown in Fig. 3d (i) and (ii), respectively. Compared with unloaded EVs in the same sample preparation, a significant enhancement of SSC signal was observed for Dox-loaded EVs as the encapsulation of Dox into the EV lumen increases the refractive index of EVs. Meanwhile, a nearly three orders of magnitude variation in Dox fluorescence is identified for Dox-loaded EVs.

Then the optimal Dox concentration for EV loading was examined by varying the Dox concentration from 5 to 300 μM. The bar graph shown in Fig. 3e for the encapsulation ratio indicates that the encapsulation ratio increased initially with the increase of Dox concentration and then reached a plateau around ~ 50% at 100 μM. Further increase of the Dox concentration till 300 μM did not achieve a higher encapsulation ratio. Compared to the ~ 80% of EV purity, the ~ 50% of encapsulation ratio indicates that not all the EVs were loaded with Dox. On the other hand, since it has been reported that Dox could insert into double-stranded DNA (dsDNA) [35], evidence needs to be obtained to exclude the scenario that Dox was bound to dsDNA on the EV surface instead of being loaded inside the lumen of EVs. A membrane-permeable nucleic acid dye, SYTO 82, was used to stain both the surface and internal DNA of EVs before and after using DNase I to digest external EV-DNA [30]. As shown in the bivariate dot plots of SYTO 82 fluorescence versus SSC (Fig. S1), the SYTO 82 staining ratio decreased from 60.3 to 39.8% after using DNase I to eradicate DNA attached to the external surface of native EVs. These results confirmed the existence of dsDNA on the EV surface, which agreed well with our previous report [30]. Then, DNase I was used to digest external EV-DNA of Dox-loaded EVs. The comparable Dox encapsulation ratio of 46.3% and 45.6% shown in the bivariate dot plots of Dox-loaded EVs without or with DNase I treatment suggests that Dox was mainly loaded into the EV lumen rather than inserting into the dsDNA on the surface of EVs (Fig. 3b, f).

Then, five other drug-loading strategies were compared with that of coincubation, including extrusion, freeze-thawing, sonication, and surfactant treatment (Triton X-100 and Tween-20) using 100 μM Dox. The Dox encapsulation ratio was measured by nFCM. Figs. 3g and S2a indicate that coincubation exhibited the highest encapsulation ratio of 48.7% followed by electroporation of 43.2%. The average encapsulation ratios for three replicate samples obtained by extrusion, freeze-thawing, sonication, and treatment by two surfactants of Triton

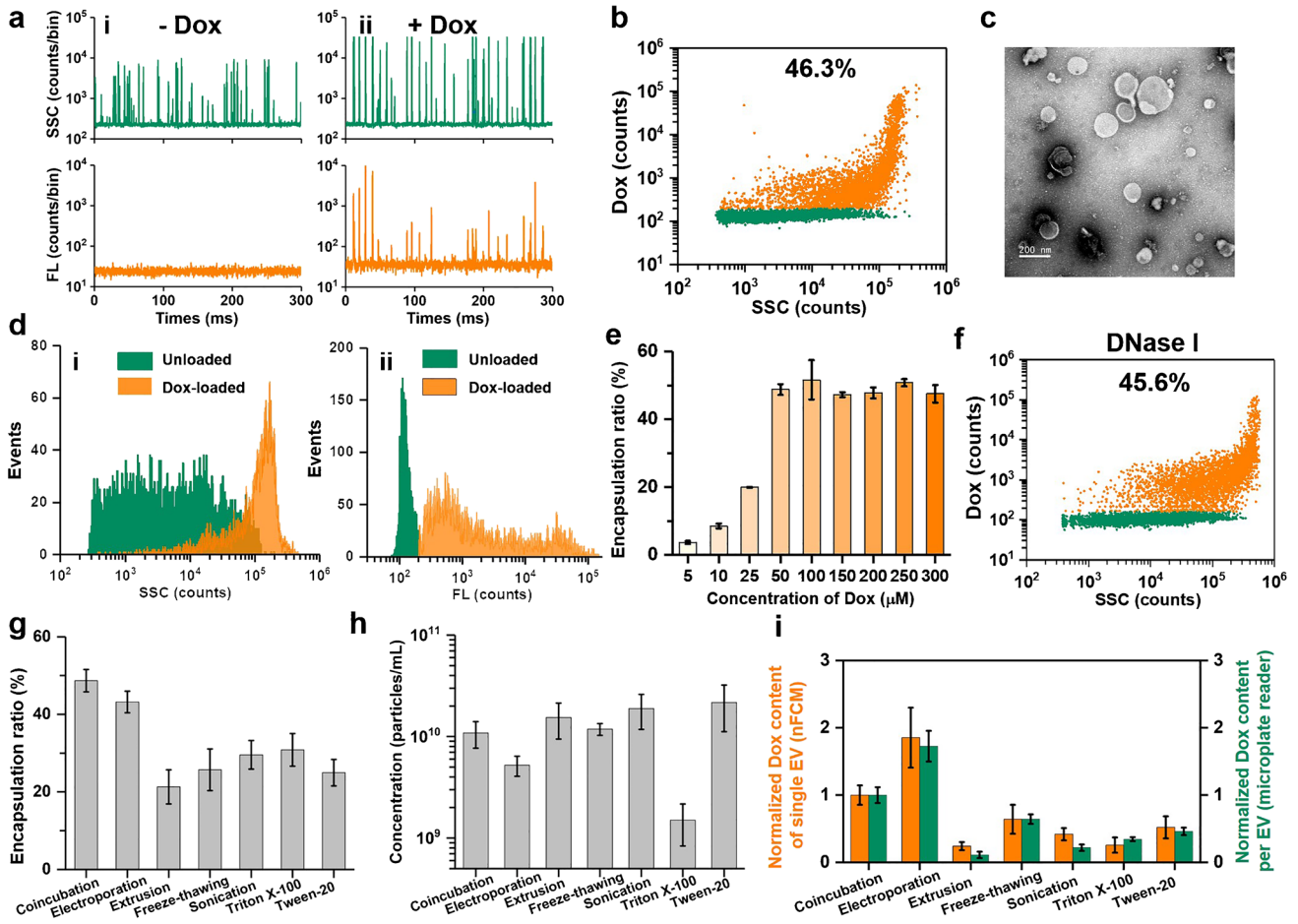

Fig. 3 Comparison of different strategies for loading Dox into EVs by nFCM. **a** Representative SSC and FL burst traces of the native EVs (i) and Dox-loaded EVs prepared by coincubation (ii). **b** The bivariate dot plot of Dox fluorescence versus SSC of Dox-loaded EVs prepared by coincubation. **c** Representative TEM micrograph of Dox-loaded EVs by coincubation; the scale bar is 200 nm. **d** SSC (i) and FL (ii) distribution histograms of native EVs and Dox-loaded EVs prepared by coincubation. **e** Optimization of the Dox concentration for loading into EVs by coincubation. **f** The bivariate dot plot of Dox fluorescence versus SSC of Dox-loaded EVs prepared by coincubation upon using DNase I to eradicate DNA attached to the external surface of EVs. **g** Encapsulation ratio of Dox for different loading strategies. **h** Particle concentrations of Dox-loaded EVs prepared by different loading strategies. **i** Dox-loading quantity assessment by single EV analysis by nFCM and ensemble-averaged analysis by a microplate reader

X-100 and Tween-20 were 21.3%, 25.7%, 29.6%, 30.8%, and 25.0%, respectively. It is interesting to note that the results measured by single-particle analysis are quite different from those obtained by ensemble-averaged approaches, of which coincubation was considered as an inefficient drug-loading approach [13]. Single-particle analysis by nFCM can objectively eliminate the potential interference of residual free drugs that co-exist with EVs upon separation, which could be overlooked by bulk analysis and lead to an overestimation of drug-loading efficiency. To note, it has been reported that the loading efficiency of targeting molecules is not only dependent on the hydrophobic nature and molecular weight of the molecules, but also influenced by the physicochemical property of EVs including lipid composition, membrane proteins, and interior solution conditions [11]. Thus, horizontal comparison under the same conditions is recommended for a rigorous conclusion.

Owing to the potential damage to EVs during the drug-loading process, particle concentrations of Dox-loaded EVs were measured by nFCM via single-particle enumeration. By using 100-nm FluoSpheres with known concentration as the external standard, the particle concentration of EVs can be calculated via the equation $C_E = (N_E/N_F) \times C_F$, where C_E, C_F, N_E, and N_F represent the EV concentration, the FluoSphere concentration, the event number of EVs counted in 1 min, and the event number of FluoSphere counted in 1 min, respectively [36]. Figure 3h shows the particle concentration of Dox-loaded EVs obtained with different drug-loading

approaches. A slight increase in particle concentration was observed for extrusion, sonication, and Tween-20 treatment as compared with that of simple coincubation. Treatment by extrusion and sonication might transform large multi-lamellar EVs into more numbers of smaller unilamellar EVs with rearrangement of vesicular lipid compositions, as described commonly for liposome production [37]. For Tween-20 treatment, the increased particle concentration could be explained by the reduction of EV absorption to the surface of tubes during the Dox-loading and removing process [38]. Meanwhile, freeze-thawing had almost no influence on the EV particle concentration. On the contrary, the particle concentration decreased upon electroporation and especially after Triton X-100 treatment. For electroporation, the decrease of EV concentration might be attributed to the fusion of EVs during the stimulation of an external electric field [39]. As a stronger surfactant compared to Tween-20, Triton X-100 is usually used to lysis the membrane structure of EVs [40]. TEM image verified that after being treated with 0.1% Triton X-100 at RT for 10 min, the EV membrane could be damaged and, thus, the particle concentration decreased during the removal of free drugs. Figure S2b indicates that similar to the native EVs, EVs loaded with Dox by coincubation, electroporation, extrusion, freeze-thawing, sonication, or Tween-20 treatment showed typical cup-shaped morphology and membrane integrity.

To further assess the Dox-loading capacity of these approaches, the Dox-loading amounts measured by nFCM were compared with those acquired using a microplate reader. Figure 3i shows the normalized median fluorescence intensity of Dox-loaded EVs subpopulation in the preparations obtained by different loading strategies in comparison with simple coincubation. Single-particle analysis by nFCM revealed that the quantity of Dox loaded into EVs by electroporation was 1.85 ± 0.45-fold of that by coincubation, while extrusion, freeze-thawing, sonication, Triton X-100 treatment, and Tween-20 treatment loaded 22%, 57%, 40%, 27%, and 32%, respectively, of the Dox quantity loaded by coincubation. Meanwhile, the same batch of Dox-loaded EVs were lysed and analyzed by a microplate reader. The Dox-loading quantity per single EV for different loading strategies is plotted in Fig. 3i for comparison. Clearly, similar results were obtained between nFCM and microplate reader measurement. Overall, in view of the encapsulation ratio, particle concentration, and Dox content, coincubation and electroporation yielded good performance for loading Dox into EVs, whereas approaches such as extrusion, freeze-thawing, sonication, and surfactant treatment are not recommended.

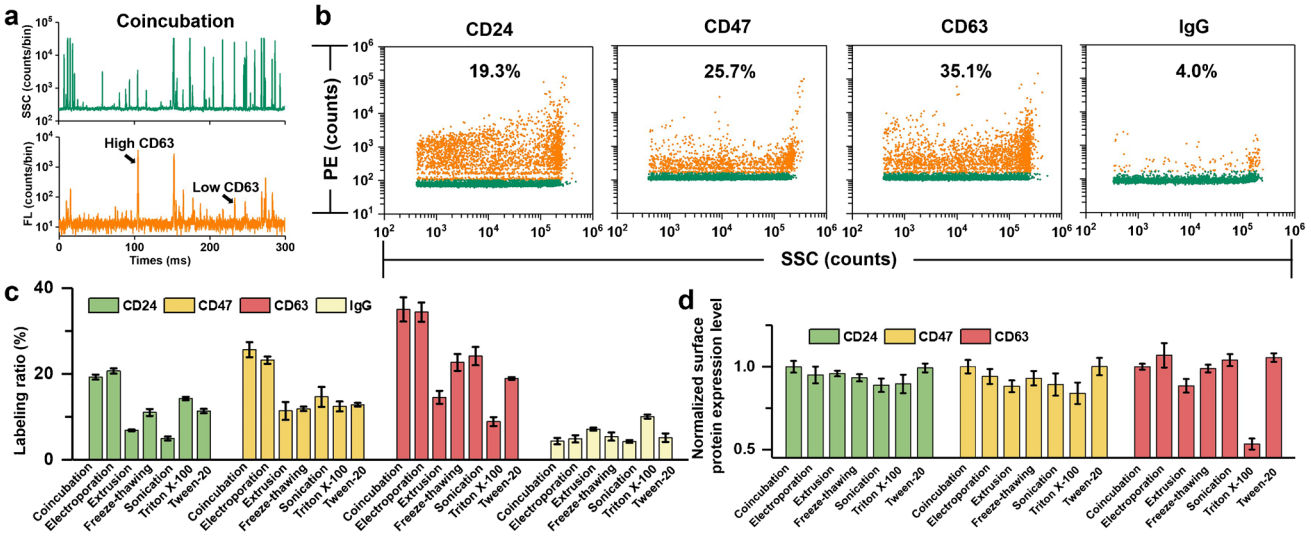

Fig. 4 Membrane protein profiling for Dox-loaded EVs prepared by different drug-loading strategies by nFCM at the single-particle level. **a** Representative SSC and FL burst traces of Dox-loaded EVs by coincubation upon CD63-PE labeling. **b** Bivariate dot plots of PE fluorescence versus SSC of different membrane proteins for Dox-loaded EVs prepared by coincubation. **c** Ratios of CD24-, CD47-, and CD63-positive EVs for Dox-loaded EVs prepared by different drug-loading strategies ($n = 3$, mean ± s.d.). **d** Normalized surface protein expression level (median fluorescence) of single EVs for Dox-loaded EVs prepared by different drug-loading strategies ($n = 3$, mean ± s.d.)

Membrane protein profiling after Dox-loading process

It has been well recognized that EVs are capable of evading immune clearance in vivo and have long circulation time due to the expression of some membrane proteins such as CD24 and CD47 [16, 41]. To take the full advantage of EVs, mild drug-loading treatment with minimal damage to these membrane proteins is highly preferred. Here, EV membrane protein profiling of CD24, CD47, and CD63 was conducted by nFCM via immunofluorescent staining to investigate the extent of protein damage after the drug-loading process. Representative SSC and FL burst traces of Dox-loaded EVs by coincubation upon CD63-PE labeling are shown in Fig. 4a, demonstrating varying expression levels of CD63 for individual EVs. The bivariate dot plots of PE fluorescence versus SSC indicate that the percentages of CD24-, CD47-, and CD63-positive EVs were 19.3%, 25.7%, and 35.1%, respectively (Fig. 4b). Meanwhile, the negative control of IgG generated a positive ratio of 4.0%. The labeling ratios of these three membrane proteins along with the IgG control for Dox-loaded EVs obtained with six different drug-loading strategies are plotted in Fig. 4c. Clearly, electroporation resulted in nearly the same performance as compared with coincubation, indicating well-preserved membrane proteins of EVs (Figs. 4c and S3). Of note, the ratios of CD24-, CD47-, and CD63-positive EVs for Dox-loaded EVs prepared by extrusion, freeze-thawing, sonication, Triton X-100 treatment, and Tween-20 treatment all exhibited different degrees of decline. For CD24, CD47, and CD63, the observed percentages of reduction were 5.0–14.3%, 11.0–14.3%, and 10.9–26.2%, respectively.

Besides, the normalized median fluorescence intensities of protein-positive EVs are plotted for each membrane protein for the Dox-loaded EV sample prepared by different loading strategies (Fig. 4d). We can see that electroporation, freeze-thawing, and Tween-20 treatment maintained approximately the same expression level for all three CD markers as compared with coincubation. For extrusion, the decrease of membrane protein quantity could result from membrane rearrangement or membrane damage when EVs were squeezing across the PC membrane for multiple cycles by extrusion force. As for surfactant treatment, depending on the treatment condition, membrane permeabilization may also interfere with the structures of membrane proteins and give rise to the decrease of labeling. Meanwhile, we noticed an increased ratio of IgG control for Triton X-100 treatment as compared with other methods (Fig. 4c), suggesting that IgG-PE could have entered into EV lumen and there could exist potential leakage of internal cargos upon membrane rupture. These speculations can be supported by the particle concentration reduction upon Triton X-100 treatment (Fig. 3h). In conclusion, considering both the labeling ratio and immunofluorescence of single EVs, coincubation and electroporation are recommended for loading Dox into EVs as the EV membrane proteins can be maintained to support the downstream EV-based therapeutic treatment.

Evaluation of the storage stability of Dox-loaded EVs

As a promising drug delivery system, whether Dox-loaded EVs can be stored for a long time is of great concern. It is essential that EV functionality and therapeutic effect can be maintained upon storage. Toward this end, Dox-loaded EVs prepared using the aforementioned different loading approaches were stored in tubes at 4 °C or – 80 °C. The encapsulation ratio was analyzed by nFCM at different time points from day 1 (the day of preparation) to day 28. We can see from Fig. 5 that the encapsulation ratio generally exhibited a downward trend with the extension of storage duration for every loading strategy, no matter if the storage temperature was at 4 °C or – 80 °C. A decrease of the encapsulation ratio can be observed as early as day 3 (the first time node for observation), suggesting a potential leakage of Dox from the lumen to the exterior of EVs. When being stored at 4 °C, the encapsulation ratios reached a plateau around day 5 or day 7 for all the six different Dox-loading approaches tested. If being stored at – 80 °C, a plateau was reached as early as day 3, and a more dramatic decrease of the encapsulation ratio was observed.

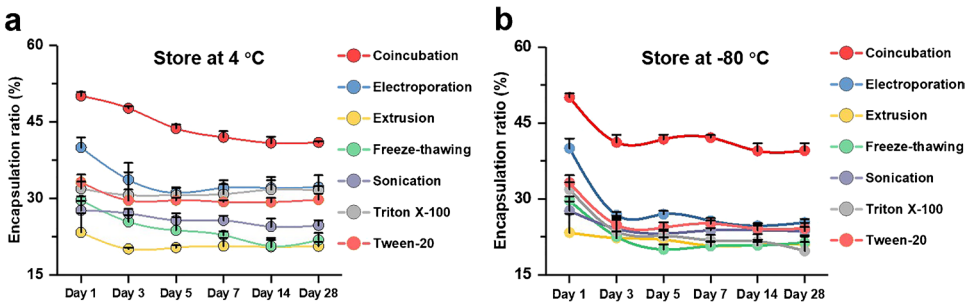

Fig. 5 Analysis of the storage stability of Dox-loaded EVs prepared by different drug-loading strategies. **a** Samples were stored at 4 °C. **b** Samples were stored at – 80 °C. Three replicates were conducted ($n = 3$, mean ± s.d.). Note that for a clearer presentation, only the upper half part of the error bars is plotted

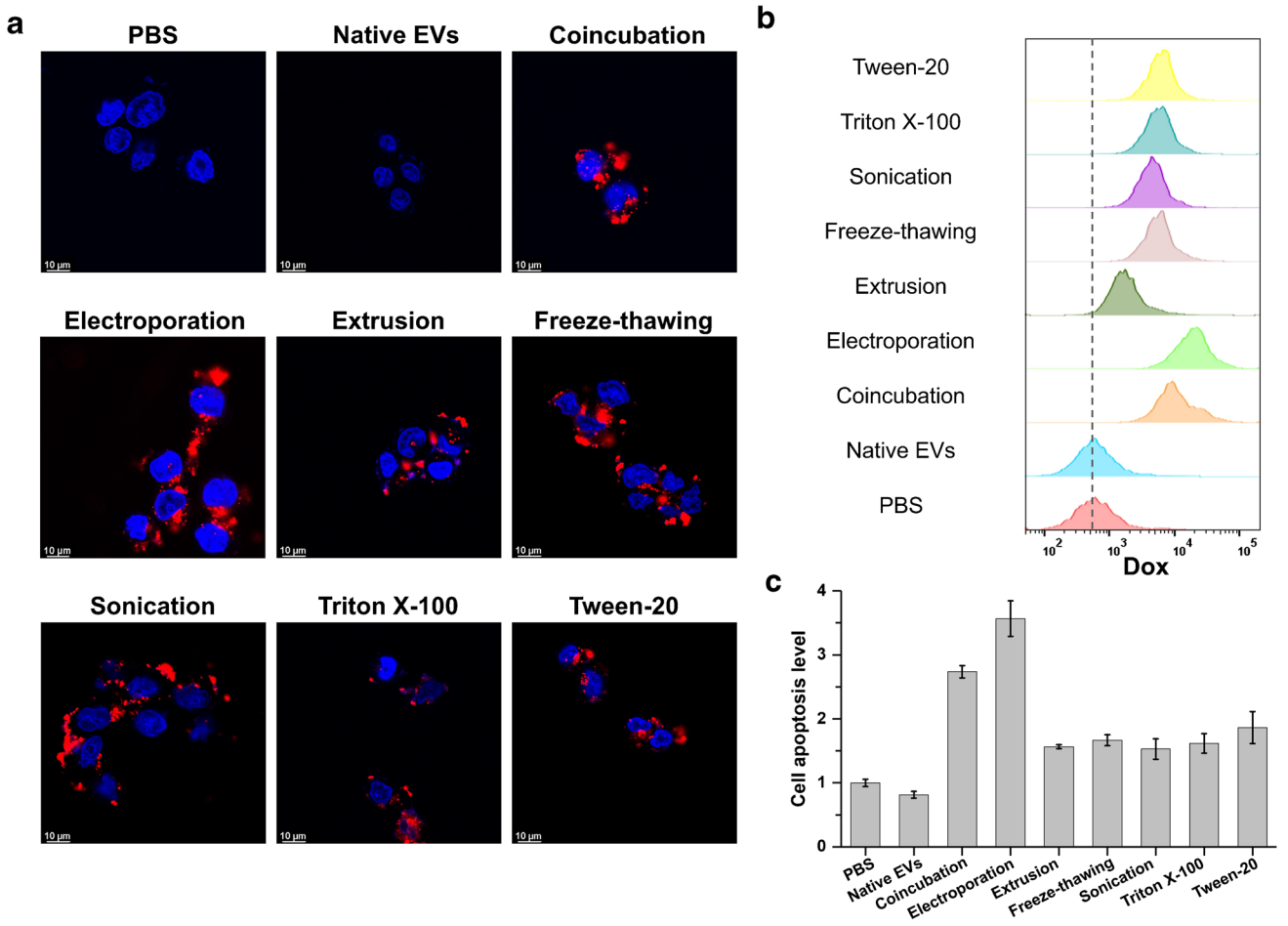

Fig. 6 Cellular internalization and apoptosis analysis. **a** Visualization of cellular uptake of DOX-loaded EVs (red) into HCT-15 cells. The cellular nuclei were stained with Hoechst 33,342 (blue). The scale bars were 10 μm. **b** FCM analysis of the fluorescence intensity of Dox for HCT-15 cells incubated with Dox-loaded EVs prepared by different drug-loading strategies. **c** Apoptosis measurements for Dox-loaded EVs ($n = 3$, mean ± SD). All the particle concentrations of Dox-loaded EVs were equivalent to the native EVs

Nevertheless, Dox-loaded EVs prepared by simple coincubation maintained the highest encapsulation ratio of nearly 40% after 28 days of storage at 4 °C or − 80 °C. In summary, Dox-loaded EVs prepared by coincubation demonstrated the highest encapsulation ratio as compared with other drug-loading strategies. Compared with − 80 °C, it is recommended to store Dox-loaded EVs at 4 °C regardless of the drug-loading methods.

Cell internalization and apoptosis measurements

Since the alternation of EV membrane integrity and proteins induced by the drug-loading process may affect the cellular internalization of EVs [42], we studied the performance of cell internalization by incubating Dox-loaded EVs with HCT-15 cells. Note that identical particle concentrations of Dox-loaded EVs were used despite their different loading approaches. Confocal images shown in Fig. 6a indicate that Dox-loaded EVs were taken up into cells for samples prepared by different loading strategies. Quantitative data revealed by FCM analysis indicated that electroporation yielded the highest cellular uptake rate and followed by coincubation (Fig. 6b). These results correlated well with the encapsulation efficiency (taking both the encapsulation ratio and drug content in single EVs into account) of EVs revealed by nFCM (Fig. 3g, i). Next, a cell apoptosis study was carried out, and the percentage of Annexin V–positive cells was used to investigate the therapeutic performance of Dox-loaded EVs (Fig. 6c). Compared to PBS and native EVs, Dox-loaded EVs prepared by all different drug-loading strategies induced obvious apoptosis. Among these, Dox-loaded EVs prepared by electroporation and coincubation showed the most significant effect

in inducing apoptosis as compared with other methods. Therefore, the therapeutic effect of Dox-loaded EVs correlated well the cellular uptake rate and fundamentally with the Dox encapsulation efficiency, implicating the veracity and significance of using nFCM for EV drug-loading characterization at the single-particle level.

Conclusions

In present study, we made a relatively comprehensive assessment of six different drug-loading strategies for incorporating Dox into EVs at the single-particle level by nFCM. The experimental results indicated that the Dox-loaded EVs prepared by coincubation and electroporation possessed a higher encapsulation ratio and more Dox content in single EVs. Correspondingly, confocal fluorescence microscopy and flow cytometry analysis revealed that Dox-loaded EVs prepared by these two procedures resulted in a higher level of cellular uptake and induced more significant apoptosis for tumor cells as compared with other drug-loading strategies. Meanwhile, Dox-loaded EVs prepared by coincubation showed the best performance upon storage at 4 °C or − 80 °C. nFCM could serve as an efficient platform for single-particle assessment of drug incorporation into EVs to promote the development of EV-based therapeutics.

Supplementary Information The online version contains supplementary material available at https://doi.org/10.1007/s00216-022-04248-4.

Funding This work was supported by the National Natural Science Foundation of China (21934004 and 21627811) and the National Key R&D Program of China (2021YFA0909400).

Declarations

Conflict of interest Xiaomei Yan has commercial interest as a co-founder of NanoFCM Inc., a company committed to commercializing the nano-flow cytometry (nFCM) technology. The other authors declare that they have no conflict of interest.

References

1. Tkach M, Thery C. Communication by extracellular vesicles: where we are and where we need to go. Cell. 2016;164(6):1226–32.
2. Jeppesen DK, Fenix AM, Franklin JL, Higginbotham JN, Zhang Q, Zimmerman LJ, Liebler DC, Ping J, Liu Q, Evans R, et al. Reassessment of exosome composition. Cell. 2019;177(2):428–45.
3. Mathieu M, Martin-Jaular L, Lavieu G, Thery C. Specificities of secretion and uptake of exosomes and other extracellular vesicles for cell-to-cell communication. Nat Cell Biol. 2019;21(1):9–17.
4. Kalluri R, Lebleu VS. The biology, function, and biomedical applications of exosomes. Science. 2020;367(6478):eaau6977.
5. Van Niel G, D'angelo G, Raposo G. Shedding light on the cell biology of extracellular vesicles. Nat Rev Mol Cell Bio. 2018;19(4):213–28.
6. De Jong OG, Kooijmans SaA, Murphy DE, Jiang L, Evers MJW, Sluijter JPG, Vader P, Schiffelers RM. Drug delivery with extracellular vesicles: from imagination to innovation. Acc Chem Res. 2019;52(7):1761–1770.
7. Nam GH, Choi Y, Kim GB, Kim S, Kim SA, Kim IS. Emerging prospects of exosomes for cancer treatment: from conventional therapy to immunotherapy. Adv Mater. 2020;32(51): e2002440.
8. Zhang X, Zhang H, Gu J, Zhang J, Shi H, Qian H, Wang D, Xu W, Pan J, Santos HA. Engineered extracellular vesicles for cancer therapy. Adv Mater. 2021;33(14): e2005709.
9. Chen J, Tan Q, Yang Z, Jin Y. Engineered extracellular vesicles: potentials in cancer combination therapy. J Nanobiotechnology. 2022;20(1):132.
10. Zhang G, Huang X, Xiu H, Sun Y, Chen J, Cheng G, Song Z, Peng Y, Shen Y, Wang J, et al. Extracellular vesicles: natural liver-accumulating drug delivery vehicles for the treatment of liver diseases. J Extracell Vesicles. 2020;10(2): e12030.
11. Fuhrmann G, Serio A, Mazo M, Nair R, Stevens MM. Active loading into extracellular vesicles significantly improves the cellular uptake and photodynamic effect of porphyrins. J Control Release. 2015;205:35–44.
12. Gao Y, Zhang H, Zhou N, Xu P, Wang J, Gao Y, Jin X, Liang X, Lv J, Zhang Y, et al. Methotrexate-loaded tumour-cell-derived microvesicles can relieve biliary obstruction in patients with extrahepatic cholangiocarcinoma. Nat Biomed Eng. 2020;4(7):743–53.
13. Hettich BF, Bader JJ, Leroux JC. Encapsulation of hydrophilic compounds in small extracellular vesicles: loading capacity and impact on vesicle functions. Adv Healthc Mater. 2022;11(5): e2100047.
14. Lee R, Ko HJ, Kim K, Sohn Y, Min SY, Kim JA, Na D, Yeon JH. Anti-melanogenic effects of extracellular vesicles derived from plant leaves and stems in mouse melanoma cells and human healthy skin. J Extracell Vesicles. 2020;9(1):1703480.
15. Zhong J, Xia BZ, Shan SB, Zheng AP, Zhang SW, Chen JG, Liang XJ. High-quality milk exosomes as oral drug delivery system. Biomaterials. 2021;277: 121126.
16. Kamerkar S, Lebleu VS, Sugimoto H, Yang S, Ruivo CF, Melo SA, Lee JJ, Kalluri R. Exosomes facilitate therapeutic targeting of oncogenic kras in pancreatic cancer. Nature. 2017;546(7659):498–503.
17. Haney MJ, Klyachko NL, Zhaoa YL, Gupta R, Plotnikova EG, He ZJ, Patel T, Piroyan A, Sokolsky M, Kabanov AV, et al. Exosomes as drug delivery vehicles for Parkinson's disease therapy. J Control Release. 2015;207:18–30.
18. De Castilla PEM, Tong LJ, Huang CY, Sofias AM, Pastorin G, Chen XY, Storm G, Schiffelers RM, Wang JW. Extracellular vesicles as a drug delivery system: a systematic review of preclinical studies. Adv Drug Deliver Rev. 2021;175: 113801.
19. Wang J, Chen D, Ho EA. Challenges in the development and establishment of exosome-based drug delivery systems. J Control Release. 2021;329:894–906.
20. Tian Y, Li S, Song J, Ji T, Zhu M, Anderson GJ, Wei J, Nie G. A doxorubicin delivery platform using engineered natural membrane vesicle exosomes for targeted tumor therapy. Biomaterials. 2014;35(7):2383–90.
21. Gandham S, Su X, Wood J, Nocera AL, Alli SC, Milane L, Zimmerman A, Amiji M, Ivanov AR. Technologies and standardization in research on extracellular vesicles. Trends Biotechnol. 2020;38(10):1066–98.
22. Willms E, Cabanas C, Mager I, Wood MJA, Vader P. Extracellular vesicle heterogeneity: subpopulations, isolation techniques, and diverse functions in cancer progression. Front Immunol. 2018;9:738.
23. Herrmann IK, Wood MJA, Fuhrmann G. Extracellular vesicles as a next-generation drug delivery platform. Nat Nanotechnol. 2021;16(7):748–59.

24. Zhu SB, Ma L, Wang S, Chen CX, Zhang WQ, Yang LL, Hang W, Nolan JP, Wu LN, Yan XM. Light-scattering detection below the level of single fluorescent molecules for high-resolution characterization of functional nanoparticles. ACS Nano. 2014;8(10):10998–1006.
25. Chen CX, Zhu SB, Wang S, Zhang WQ, Cheng Y, Yan XM. Multiparameter quantification of liposomal nanomedicines at the single-particle level by high-sensitivity flow cytometry. Acs Appl Mater Inter. 2017;9(16):13913–9.
26. Tian Y, Ma L, Gong MF, Su GQ, Zhu SB, Zhang WQ, Wang S, Li ZB, Chen CX, Li LH, et al. Protein profiling and sizing of extracellular vesicles from colorectal cancer patients via flow cytometry. ACS Nano. 2018;12(1):671–80.
27. Tian Y, Gong MF, Hu YY, Liu HS, Zhang WQ, Zhang MM, Hu XX, Aubert D, Zhu SB, Wu L, et al. Quality and efficiency assessment of six extracellular vesicle isolation methods by nano-flow cytometry. J Extracell Vesicles. 2020;9(1):1697028.
28. Chen C, Sun M, Wang J, Su L, Lin J, Yan X. Active cargo loading into extracellular vesicles: highlights the heterogeneous encapsulation behaviour. J Extracell Vesicles. 2021;10(13): e12163.
29. Chen CX, Sun MD, Liu X, Wu WJ, Su LY, Li YM, Liu G, Yan XM. General and mild modification of food-derived extracellular vesicles for enhanced cell targeting. Nanoscale. 2021;13(5):3061–9.
30. Liu HS, Tian Y, Xue CF, Niu Q, Chen C, Yan XM. Analysis of extracellular vesicle DNA at the single-vesicle level by nano-flow cytometry. J Extracell Vesicles. 2022;11(4): e12206.
31 Liu HS, Yuan WL, Pang QS, Xue CF, Yan XM. Single-particle analysis of tear fluid reveals abundant presence of tissue factor-exposing extracellular vesicles with strong coagulation activity. Talanta. 2022;239:123089.
32. Yang LL, Zhu SB, Hang W, Wu L, Yan XM. Development of an ultrasensitive dual-channel flow cytometer for the individual analysis of nanosized particles and biomolecules. Anal Chem. 2009;81(7):2555–63.
33. Zhu SB, Yang LL, Long Y, Gao M, Huang TX, Hang W, Yan XM. Size differentiation and absolute quantification of gold nanoparticles via single particle detection with a laboratory-built high-sensitivity flow cytometer. J Am Chem Soc. 2010;132(35):12176–8.
34. Thery C, Witwer KW, Aikawa E, Alcaraz MJ, Anderson JD, Andriantsitohaina R, Antoniou A, Arab T, Archer F, Atkin-Smith GK, et al. Minimal information for studies of extracellular vesicles 2018 (misev2018): a position statement of the International Society for Extracellular Vesicles and update of the misev2014 guidelines. J Extracell Vesicles. 2018;7(1):1535750.
35. Yao F, Duan J, Wang Y, Zhang Y, Guo Y, Guo H, Kang X. Nanopore single-molecule analysis of DNA-doxorubicin interactions. Anal Chem. 2015;87(1):338–42.
36. Niu Q, Ma L, Zhu S, Li L, Zheng Q, Hou J, Lian H, Wu L, Yan X. Quantitative assessment of the physical virus titer and purity by ultrasensitive flow virometry. Angew Chem Int Ed Engl. 2021;60(17):9351–6.
37. Large DE, Abdelmessih RG, Fink EA, Auguste DT. Liposome composition in drug delivery design, synthesis, characterization, and clinical application. Adv Drug Deliver Rev. 2021;176: 113851.
38. Van De Wakker SI, Van Oudheusden J, Mol EA, Roefs MT, Zheng W, Gorgens A, El Andaloussi S, Sluijter JPG, Vader P. Influence of short term storage conditions, concentration methods and excipients on extracellular vesicle recovery and function. Eur J Pharm Biopharm. 2022;170:59–69.
39. Johnsen KB, Gudbergsson JM, Skov MN, Christiansen G, Gurevich L, Moos T, Duroux M. Evaluation of electroporation-induced adverse effects on adipose-derived stem cell exosomes. Cytotechnology. 2016;68(5):2125–38.
40. Ahyayauch H, Bennouna M, Alonso A, Goni FM. Detergent effects on membranes at subsolubilizing concentrations: transmembrane lipid motion, bilayer permeabilization, and vesicle lysis/reassembly are independent phenomena. Langmuir. 2010;26(10):7307–13.
41. Yu Y, Gool E, Berckmans RJ, Coumans FaW, Barendrecht AD, Maas C, Van Der Wel NN, Altevogt P, Sturk A, Nieuwland R. Extracellular vesicles from human saliva promote hemostasis by delivering coagulant tissue factor to activated platelets. J Thromb Haemost. 2018;16(6):1153–1163.
42. Mulcahy LA, Pink RC, Carter DR. Routes and mechanisms of extracellular vesicle uptake. J Extracell Vesicles. 2014;3:24641.

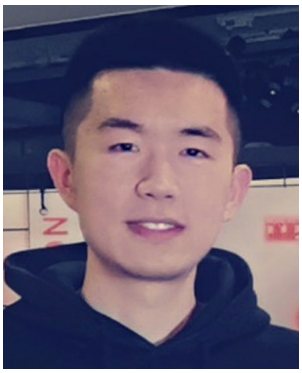

Chen Chen is a PhD candidate in Prof. Xiaomei Yan's group in the College of Chemistry and Chemical Engineering at Xiamen University. His research focused on the characterization and application of drug-loaded liposomes and extracellular vesicles.

Yurou Li is a master's degree student in Prof. Xiaomei Yan's group in the College of Chemistry and Chemical Engineering at Xiamen University. In her research, she focused on the application of engineered extracellular vesicles for drug delivery.

Qingqing Wang is a master's degree student in Prof. Xiaomei Yan's group in the College of Chemistry and Chemical Engineering at Xiamen University where she focuses on the study of the toxin-antitoxin system and their effects on bacterial persistence and resistance.

Niangui Cai is a PhD graduate student in Prof. Xiaomei Yan's group in the College of Chemistry and Chemical Engineering at Xiamen University. His research focuses on the characterization of EV surface glycosylation and the application of extracellular vesicles in nanomedicine.

Lina Wu is an associate professor in the College of Chemistry and Chemical Engineering at Xiamen University. Her research interest is focused on the specific detection of bacteria using engineered bacteriophages as well as the toxin-antitoxin system study and cell cycle analysis of bacteria.

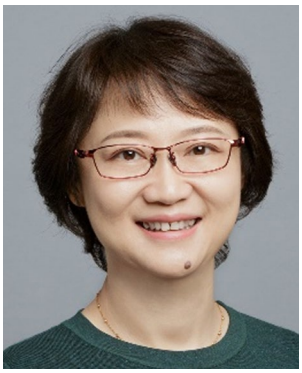

Xiaomei Yan is a distinguished professor in the College of Chemistry and Chemical Engineering at Xiamen University. She is interested in the development of advanced instrumentation and methodologies for bioanalysis. In particular, she has developed nano-flow cytometry to address the challenges of quantitative physical and biochemical characterization of single nanoparticles such as extracellular vesicles, bacteria, viruses, mitochondria, and nanomedicines.